# Very Small Bandgap π-Conjugated Polymers with Extended Thienoquinoids

Kohsuke Kawabata,*,[†] Masahiko Saito,[†] Itaru Osaka,*,[†] and Kazuo Takimiya[†]

[†]Emergent Molecular Function Research Group, Center for Emergent Matter Science, RIKEN, Wako, Saitama 351-0198, Japan
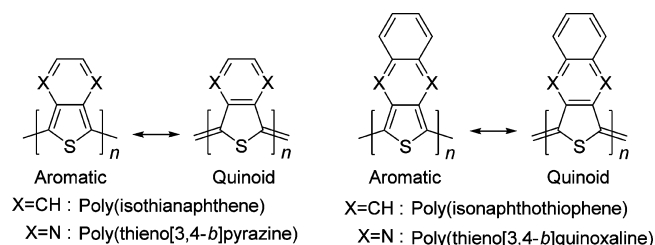
S *Supporting Information*

ABSTRACT: The introduction of quinoidal character to π-conjugated polymers is one of the effective approaches to reducing the bandgap. Here we synthesized new π-conjugated polymers (**PBTD4T** and **PBDTD4T**) incorporating thienoquinoids 2,2'-bithiophene-5,5'-dione (BTD) and benzo[1,2-*b*:4,5-*b*']-dithiophene-2,6-dione (BDTD) as strong electron-deficient (acceptor) units. **PBTD4T** showed a deep LUMO energy level of −3.77 eV and a small bandgap of 1.28 eV, which are similar to those of the analog using thieno[3,2-*b*]thiophene-2,5-dione (TTD) (**PTTD4T**). **PBDTD4T** had a much deeper LUMO energy level of −4.04 eV and a significantly smaller bandgap of 0.88 eV compared to those of the other two polymers. Interestingly, **PBDTD4T** showed high transparency in the visible region. The very small bandgap of **PBDTD4T** can be rationalized by the enhanced contribution of the resonance backbone structure in which the *p*-benzoquinodimethane skeleton in the BDTD unit plays a crucial role. **PBTD4T** and **PBDTD4T** exhibited ambipolar charge transport with more balanced mobilities between the hole and the electron than **PTTD4T**. We believe that the very small bandgap, i.e., the high near-infrared activity, as well as the well-balanced ambipolar property of the π-conjugated polymers based on these units would be of particular interest in the fabrication of next-generation organic devices.
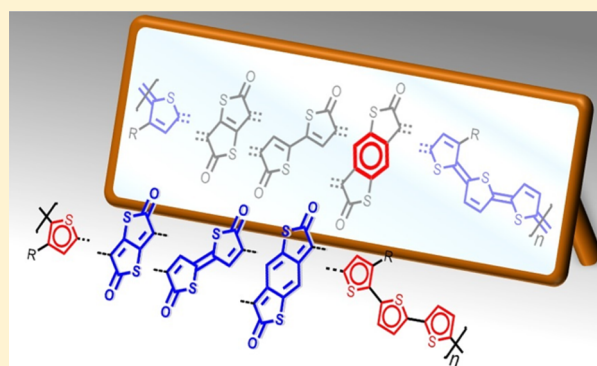
INTRODUCTION

The area of π-conjugated polymers has undergone rapid development in the last few decades most likely because if the potential application of the polymers in organic devices, such as organic light-emitting diodes (OLEDs),[1] organic field-effect transistors (OFETs),[2] organic photovoltaics (OPVs),[3] electrochromic devices,[4] transparent electrodes,[5,6] photoconductors,[7] and thermoelectrics.[8] Small bandgap π-conjugated polymers are of great interest because of their near-infrared (NIR) activity, high conductivity, and ambipolar charge transport property.[9−12] Early studies on poly(isothianaphthene)[13−15] and poly-(isonaphthothiophene)[16,17] (Figure 1) have shown that these polymers can have very small bandgaps, in which the quinoidal

character in the aromatic conjugated backbone plays an important role in reducing the bandgap.[15] It was revealed that replacing carbon atoms on the benzene ring with nitrogen atoms resulting in poly(thieno[3,4-*b*]pyrazine) and poly-(thieno[3,4-*b*]quinoxaline) can even further reduce the bandgap.[17] Notably, several groups have successfully synthesized soluble poly(thieno[3,4-*b*]pyrazine) derivatives,[18−20] which were used as the active material for OPVs.[20] Recent advances in molecular design using donor−acceptor (D−A) backbones in which electron-rich (donor) and electron-deficient (acceptor) π-building units are alternately incorporated[21−23] have enabled us to tune the bandgap and the frontier molecular orbital energy levels as well as to reduce the bandgap. This has allowed us to create more practical small bandgap polymers.[9,24]

The key to the development of small bandgap D−A polymers is the incorporation of strong acceptor units into the backbone. This markedly lowers the lowest unoccupied molecular orbital (LUMO) energy level of the polymers, thereby reducing the bandgap without raising the highest occupied molecular orbital (HOMO) energy level. The deep LUMO and HOMO energy levels are crucial for electron transport in air and chemical (oxidative) stability in air,

Figure 1. Chemical and resonance structures of poly-(isothianaphthene), poly(isonaphthothiophene), poly(thieno[3,4-*b*]-pyrazine), and poly(thieno[3,4-*b*]quinoxaline).
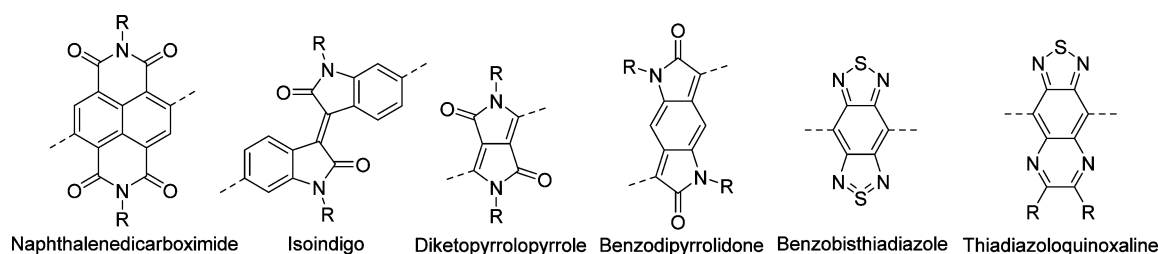
Figure 2. Typical strong acceptor units used in small bandgap π-conjugated polymers.
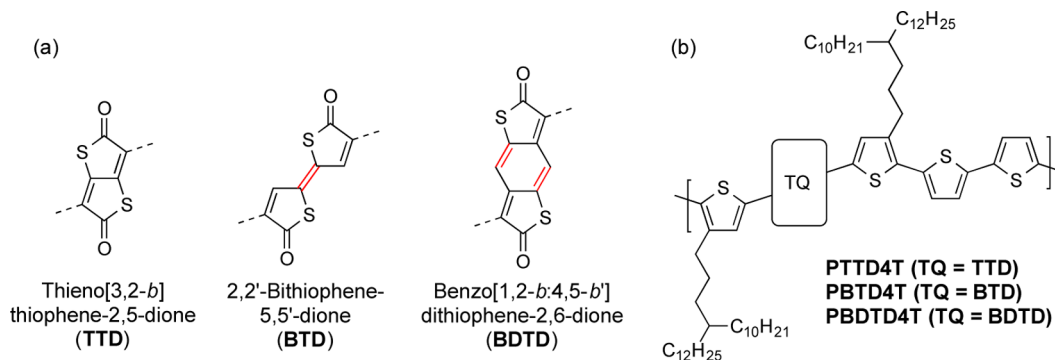
Figure 3. Chemical structures of thienoquinoidal acceptors examined in this study: (a) thieno[3,2-*b*]thiophene-2,5-dione (TTD), 2,2′-bithiophene-5,5′-dione (BTD), and benzo[1,2-*b*:4,5-*b*′]dithiophene-2,6-dione (BDTD). (b) π-Conjugated polymers incorporating the acceptors, i.e., **PTTD4T**, **PBTD4T**, and **PBDTD4T**, respectively.

respectively. With these electronic properties, D−A polymers possessing strong acceptor units function as ambipolar materials for OFETs[11,25−27] and as both p- and n-type materials for OPVs.[28−31] Typical strong acceptor units include imide- and amide-containing dyes, such as naphthalenedicarboximide,[32,33] isoindigo,[34,35] diketopyrrolopyrrole,[33] and benzodipyrrolidone,[26,36,37] and *o*-quinoidal heterocycles, such as benzobisthiadiazole[22,38] and thiadiazoloquinoxaline[11,25,39] (Figure 2).

Thienoquinoids with electron-withdrawing groups are also fascinating strong acceptor units because the molecules themselves possess small bandgaps as well as deep HOMO and LUMO energy levels thanks to the quinoid structures and the electron-withdrawing nature of the functional groups. Indeed, thienoquinoids based on oligothiophenes and acenedithiophenes with cyano and/or carbonyl groups have been reported to show immense potential as n-type and/or ambipolar organic semiconductors.[40−46] However, thienoquinoids have been rarely used as the building unit for π-conjugated polymers.

Recently, we have reported the synthesis of a series of D−A π-conjugated polymers incorporating a thienoquinoid with carbonyl termini, thieno[3,2-*b*]thiophene-2,5-dione (TTD), as the acceptor unit (Figure 3).[47,48] The incorporation of the TTD unit into the polythiophene-based backbones yielded polymers having quite small optical bandgaps (E_g's) of approximately 1.2 eV with deep LUMO energy levels (E_{LUMO}'s) of approximately −3.8 eV. These polymers also demonstrated p-channel or ambipolar behavior in OFETs depending on the device structure, with high hole mobilities of up to 1.4 cm^2 V^{-1} s^{-1} in p-channel OFETs and well-balanced hole and electron mobilities under ambient conditions in ambipolar OFETs. These interesting results have encouraged us to further investigate thienoquinoids as the building unit for π-conjugated polymers.

2,2′-Bithiophene-5,5′-dione (BTD) and benzo[1,2-*b*:4,5-*b*′]-dithiophene-2,6-dione (BDTD)[49] (Figure 3) are other examples of thienoquinoids with carbonyl termini, the quinoid structures of which are extended compared with TTD. BTD is also regarded as an isomer of S-Pechmann dye, which has been reported recently.[50] To the best of our knowledge, BTD and BDTD have not yet been investigated as building units for π-conjugated polymers. Here we synthesized two new π-conjugated polymers incorporating BTD and BDTD (**PBTD4T** and **PBDTD4T**, Figure 3). We had initially expected that with the extended structure, the incorporation of BTD and BDTD units would enhance the quinoidal character in the polymer backbone, thereby reducing the bandgap of the polymers compared with that of their TTD-based counterpart (**PTTD4T**, Figure 3). In fact, we found that although **PBTD4T** exhibited similar electronic properties to **PTTD4T**, **PBDTD4T** had an extremely reduced E_g of 0.88 eV along with a deep E_{LUMO} of approximately −4.0 eV. This difference can be explained by taking into account their resonance structures. We discuss the correlation between the molecular structures and the electronic structures of the polymers. In addition, we also show their thin-film structures and charge transport properties.

■ RESULTS AND DISCUSSION

Molecular Design and Synthesis. The backbones of the D−A polymers in this study are composed of the thienoquinoidal acceptor unit and the quaterthiophene donor unit. The simple quaterthiophene donor unit was chosen to help us better understand the nature of the acceptor units. The long branched 4-decylhexadecyl group was employed as the solubilizing alkyl group. BTD- and BDTD-based monomers (**BTD2T-Br2** and **BDTD2T-Br2**) were synthesized in a manner similar to the synthesis of the TTD analog that was previously reported (Scheme 1).[48]

Scheme 1. Synthesis of BTD- and BDTD-Based Monomers[a]
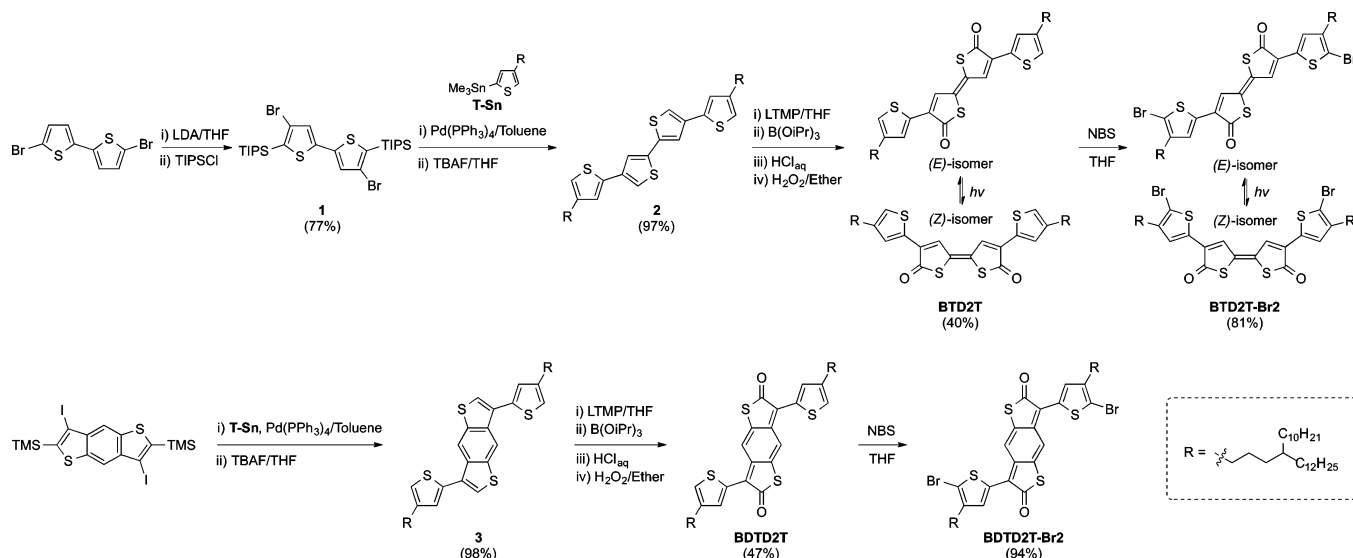
[a]LDA: lithium diisopropylamide. TIPSCl: triisopropylsilyl chloride. TBAF: tetrabutylammonium fluoride. LTMP: lithium tetramethylpiperidide. NBS: N-bromosuccinimide.

BTD2T-Br2 was synthesized from 5,5′-dibromo-2,2′-bithiophene. Initially, the dibromobithiophene was converted into 4,4′-dibromo-5,5′-bis(triisopropylsilyl)-2,2′-bithiophene (**1**) via the halogen dance reaction by using lithium diisopropylamide (LDA).[51] Then, alkylthiophenes were introduced at the β-positions of **1** via the Migita−Kosugi−Stille cross-coupling reaction with 2′-trimethylstannyl-4′-(4-decylhexadecyl)-thiophene (**T-Sn**), and the silyl groups were subsequently deprotected using tetrabutylammonium fluoride (TBAF) to give **2**. The α-positions of the bithiophene core of **2** were selectively lithiated by using lithium tetramethylpiperidide (LTMP) and then borylated with triisopropyl borate. The boronic acid groups were immediately oxidized with hydrogen peroxide to form the BTD moiety (**BTD2T**). Finally, the α-positions of the flanking alkylthiophenes of **BTD2T** were brominated with N-bromosuccinimide (NBS) to give **BTD2T-Br2**. Note that both **BTD2T** and **BTD2T-Br2** were obtained as a mixture of (E) and (Z) isomers. Interestingly, the isomerization at the central BTD unit occurred in solution under light at room temperature, which was confirmed by two-dimensional thin-layer chromatography using **BDT2T** (Figure S1). The polymerization of **BTD2T-Br2** was carried out using the mixture of (E) and (Z) isomers.

BDTD2T-Br2 was synthesized in a similar manner. First, the alkylthiophene groups were introduced at the β-positions of 2,6-bis(trimethylsilyl)-3,7-diiodobenzo[1,2-b:4,5-b′]-dithiophene, and then the silyl groups of the benzodithiophene core were deprotected to afford **3**. The quinoidation of the benzodithiophene core yielded **BDTD2T**, which was then brominated to afford **BDTD2T-Br2**.

All the monomers produced a peak around 190 ppm in the ^{13}C NMR spectra, which corresponds to the carbonyl carbon, and peaks around 1650−1700 cm^{−1} in the IR spectra, which correspond to C═O stretching. These data, in combination with ^{1}H NMR spectra, offer clear evidence of the presence of the quinoidal-dione structure in the monomers (Figure S2).

The TTD-based monomer (**TTD2T-Br2**, see the Supporting Information for the synthesis), **BTD2T-Br2**, and **BDTD2T-Br2** were then copolymerized with 5,5′-distannyl-2,2′-bithio-phene by the Migita−Kosugi−Stille polycondensation in the presence of tetrakis(triphenylphosphine)palladium(0) to afford **PTTD4T**, **PBTD4T**, and **PBDTD4T**, respectively (Scheme 2).

Scheme 2. Synthesis of Polymers
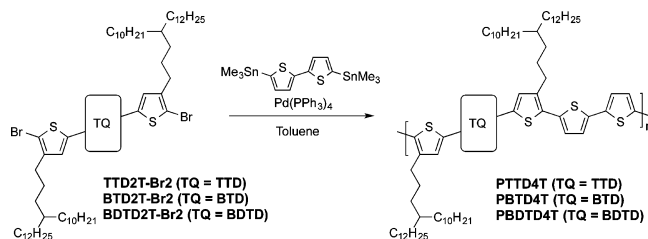
The polymers were purified by sequential Soxhlet extraction. The major products of **PTTD4T**, **PBTD4T**, and **PBDTD4T** were obtained as chlorobenzene (CB), chloroform, and o-dichlorobenzene (DCB) fractions, respectively. The number-average molecular weights (M_n) of the polymers were 48 kDa for **PTTD4T**, 37 kDa for **PBTD4T**, and 58 kDa for **PBDTD4T**, as determined by gel permeation chromatography (GPC) using DCB as the eluent at 140 °C (Table 1). The large polydispersity indexes of the polymers could be an artifact due to bimodal peaks observed in the GPC most likely caused by its strong aggregation (Figure S3). Similar behaviors are often observed in conjugated polymers that show strong aggregation.[52,53] In the IR spectra, all the polymers exhibited strong

Table 1. Polymerization Results[a]

polymer	M_n (KDa)	M_w (kDa)	M_w/M_n	DP$_n$[b]
PTTD4T	48	1883	39.3	39
PBTD4T	37	126	3.4	30
PBDTD4T	58	182	3.1	45

[a]Determined by high-temperature GPC using DCB as the eluent at 140 °C and calibrated with polystyrene standards. [b]Degree of polymerization determined on the basis of the number of repeating monomer units.

C=O stretching absorptions around 1650−1700 cm^{-1}, similar to the monomers (Figure S2). This indicates that the quinoidal−dione structure is present in the polymer backbones and that the polymerization does not affect the chemical structures of the TTD, BTD, and BDTD units. It should also be mentioned that **PBTD4T** was obtained as a mixture of (E) and (Z) isomers with an (E) to (Z) ratio of approximately 65:35, as estimated by ^{1}H NMR spectroscopy.

Electronic Structures. We investigated the electronic properties of the polymer thin films by cyclic voltammetry and UV−vis−NIR absorption spectroscopy. Figure 4 displays
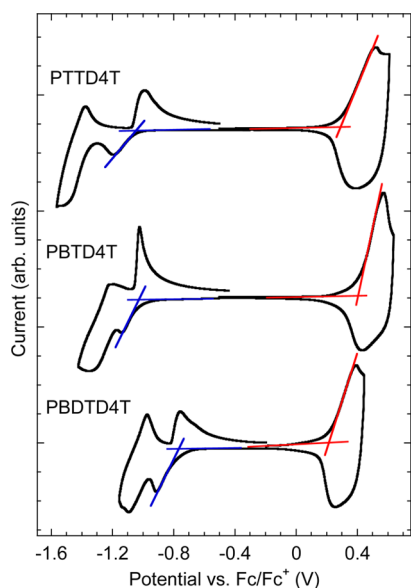

Figure 4. Cyclic voltammograms of polymer films.

the cyclic voltammograms of the polymer films. All the polymer films showed reversible one-electron oxidation and two-electron reduction current responses. HOMO energy levels (E_{HOMO}'s) and E_{LUMO}'s of the polymers were estimated from the oxidation and the first reduction onset potentials (Table 2). The E_{LUMO} of **PBTD4T** was −3.77 eV, which is similar to that of **PTTD4T** (−3.76 eV), whereas that of **PBDTD4T** was −4.04 eV, which is significantly deeper than that of **PTTD4T**. These E_{LUMO}'s would be sufficient for electron transport in ambient conditions. Thus, BTD and BDTD are indeed strong acceptor units. The E_{HOMO} of **PBTD4T** was −5.20 eV, which is deeper than that of **PTTD4T** (−5.09 eV), and that of **PBDTD4T** was −5.02 eV, which is slightly shallower than that of **PTTD4T**. As a result, **PBTD4T** and **PBDTD4T**, respectively, had a larger and a smaller HOMO−LUMO gap than **PTTD4T**, consistent with the optical bandgap (E_g)

determined from the UV−vis−NIR spectra as shown below. We also evaluated the E_{HOMO} of the polymers by photo-emission yield spectroscopy (PYS) using polymer thin films (Table 2 and Figure S5). The E_{HOMO}'s of **PTTD4T**, **PBTD4T**, and **PBDTD4T** were −5.23, − 5.44, and −5.30 eV, respectively, which would be sufficiently deep for being stable against air oxidation.

The variation of E_{HOMO} and E_{LUMO} was contrary to our expectations based on the electrochemical properties (Figure S6a and Table S1) and the DFT calculation performed at the B3LYP/6-31G(d) level (Figures S7 and S8) of the monomers (**TTD2T**, **BTD2T**, and **BDTD2T** with methyl groups instead of long branched alkyl groups). In both experiment and theory, **BTD2T** was found to have a shallower HOMO energy level and consequently a smaller HOMO−LUMO gap than **TTD2T**. One plausible reason could be the difference in the conformation of alkylthiophenes. In the optimized geometry of the trimer determined by DFT calculation, although the conformation of the carbonyl termini of the thienoquinoidal unit and the sulfur atom of the adjacent alkylthiophen was in the anti conformation for **BTD2T** and **BDTD2T**, it was syn for **TTD2T** (Figures S9 and S10). Furthermore, in the trimer of **TTD2T**, the syn conformation was found to have a smaller HOMO−LUMO gap than in the anti conformation. Thus, the difference in the dominant conformation at the bond between the thienoquinoidal unit and alkylthiophene in the polymer system could explain the smaller E_g of **PTTD4T** than **PBTD4T**.
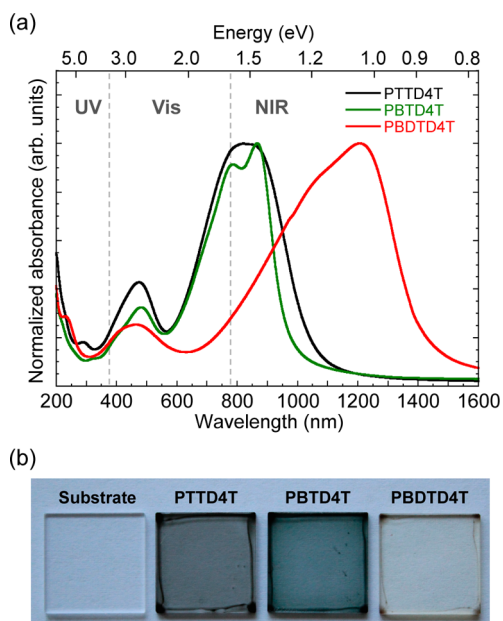
Figure 5a shows the UV−vis−NIR absorption spectra of the polymer thin films. **PBTD4T** showed a strong absorption band around 800 nm and an absorption maximum (λ_{max}) at 866 nm, similar to those of **PTTD4T**. E_g of **PBTD4T** was 1.28 eV as estimated from the absorption onset (λ_{edge} = 968 nm). This value was larger than that of **PTTD4T** (1.19 eV) despite the fact that the π-electron system of BTD is longer than that of TTD. Note that even low-molecular-weight **PBTD4T** (M_n = 13 kDa, from the hexane fraction) had a similar absorption onset (Figure S12). The effective conjugation along the backbone was already saturated at this low molecular weight; thus, the low molecular weight of **PBTD4T** compared to **PTTD4T** (Table 1) would not be a reason for the large E_g. As discussed above, the large E_g of **PBTD4T** compared to that of **PTTD4T** could be due to differences in the structural conformation. In sharp contrast, **PBDTD4T** showed a significantly red-shifted absorption band whose λ_{max} appeared at 1207 nm relative to those of **PTTD4T** and **PBTD4T**. A very small E_g of 0.88 eV (λ_{edge} = 1415 nm), which is comparable to those of recently reported π-conjugated polymers with very small E_g's, was obtained.[11,36,37,39,54−58] We note that the strong NIR absorption of **PBDTD4T** originates not in the oxidized state

Table 2. Physicochemical Properties of Polymer Films

polymer	E_{red} (V)[a]	E_{ox} (V)[a]	E_{LUMO} (eV)[b]	E_{HOMO} (eV)		λ_{max} (nm)[d]	λ_{edge} (nm)[e]	E_g (eV)[f]
				CV[b]	PYS[c]			
PTTD4T	−1.04	0.29	−3.76	−5.09	−5.23	833	1046	1.19
PBTD4T	−1.03	0.40	−3.77	−5.20	−5.44	866	968	1.28
PBDTD4T	−0.76	0.22	−4.04	−5.02	−5.30	1207	1415	0.88

[a]Reduction potential (E_{red}) and oxidation potential (E_{ox}) determined from the onset. [b]LUMO (E_{LUMO}) and HOMO (E_{HOMO}) energy levels estimated with the following equations: $E_{LUMO} = -4.80 - E_{red}$, $E_{HOMO} = -4.80 - E_{ox}$. [c]$E_{HOMO}$ estimated by photoemission yield spectroscopy. [d]Absorption maxima of polymer thin films. [e]Absorption edges of polymer thin films. [f]Optical bandgaps estimated from absorption edges of polymer thin films.

Figure 5. (a) UV−vis−NIR absorption spectra of the polymer thin films. (b) Photographs of the polymer thin films (thickness = ca. 60 nm) on quartz glass substrates. A bare quartz glass substrate is also shown on the left. The thin films were deposited by spin-coating the *o*-dichlorobenzene solution.

but in the neutral state. This was supported by the change in film absorption by the electrochemical oxidation from its neutral state. We observed the disappearance of the initial NIR absorption band around 1200 nm and a further redshift upon electrochemical oxidation, indicating the formation of a polaron band (Figure S13).

Interestingly, in **PBDTD4T**, the absorption in the visible region (380−750 nm) was significantly weak compared to that in the NIR region (>750 nm). As a result, the **PBDTD4T** film clearly showed higher transparency in visible region than those of **PTTD4T** and **PBTD4T** (Figure 5b). The strong NIR absorption and the absence of the visible absorption are of particular importance for application in NIR photodetectors or transparent electronics.[12,59−62]

As shown above, E_g of **PBDTD4T** is much smaller than those of **PTTD4T** and **PBTD4T**, and it is essential to consider the origin of this phenomenon. The trend of E_g in these polymers can be qualitatively understood by considering their resonance forms. Figure 6 illustrates the primary forms of the
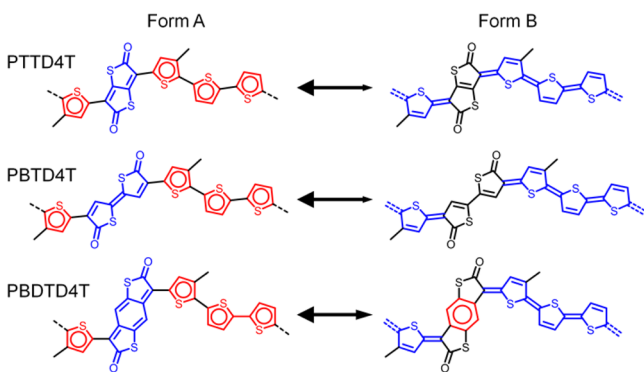

Figure 6. Two possible resonance forms of polymers. Red and blue lines indicate aromatic and quinoidal structures, respectively.

polymers (form A) and their resonance forms (form B), in which form A includes the quaterthiophene moieties with the aromatic structure and form B includes those with the quinoid structure. A clear structural difference between **PBDTD4T** and **PTTD4T/PBTD4T** was seen in form B. In form B, **PBDTD4T** has an aromatic benzene substructure in the BDTD unit, whereas **PTTD4T** and **PBTD4T** do not have an aromatic substructure in the thienoquinoidal unit. This aromatic-like structure in the BDTD unit in the resonance form can stabilize the polymer structure in form B, thereby enhancing the contribution of form B. Thus, the quinoidal character of **PBDTD4T** should be more enhanced than those of **PTTD4T** and **PBTD4T**. This could be a major origin of the significantly smaller E_g in **PBDTD4T** than in **PTTD4T** and **PBTD4T**. It is also important to note that in designing small bandgap polymers the *p*-benzoquinodimethane skeleton such as that in the BDTD unit or a similar structure that can change into an aromatic-like structure in the resonance form may play a crucial role.

To support this argument, we investigated the quinoidal character of the backbone by comparing C−C and C≡C bond lengths in the model structures obtained by DFT calculation at the B3LYP/6-31G(d) level. To reflect better the molecular structure in the polymer system, we carried out the calculation by using the model trimers and extracted the bond lengths from the central repeat units of the trimers. Figures 7a−c show the chemical structures of the repeat units of **PTTD4T**, **PBTD4T**, and **PBDTD4T**, respectively, and the plots of C−C bond length at the respective bond number. To directly compare quinoid contribution between the polymers, we focused on the bond length in the quaterthiophene moiety that is common to these polymers. In **PTTD4T** and **PBTD4T**, the inter-ring C−C bond lengths and C−C bond lengths in the thiophene rings were approximately 1.438−1.441 Å and 1.407−1.415 Å, respectively, and the C≡C bond lengths in the thiophene rings were 1.384−1.397 Å. In **PBDTD4T**, the inter-ring C−C bond lengths and C−C bond lengths in the thiophene rings were approximately 1.433−1.436 Å and 1.404−1.408 Å, respectively, and the C≡C bond lengths in the thiophene rings were 1.387−1.400 Å. As a result, the C−C bonds and C≡C bonds in the quaterthiophene moiety in **PBDTD4T** were shorter and longer than those in **PTTD4T** and **PBTD4T**, respectively. These results suggest that the quaterthiophene moiety in **PBDTD4T** has enhanced quinoidal character compared to those in **PTTD4T** and **PBTD4T**. Thus, we can safely rationalize that the very small E_g of **PBDTD4T** is ascribed to the enhanced contribution of form B.

Thin-Film Structure. To investigate the microstructures of the polymer thin films, 2D grazing incidence X-ray diffraction (2D-GIXD) measurements were carried out. Figure 8 shows the 2D-GIXD images of the annealed polymer thin films on silicon wafers and their in-plane and out-of-plane profiles. In the 2D-GIXD images, the polymer thin films furnished strong spotlike diffractions along the quasi-q_z axes, which correspond to the lamellar structures, (h00), with the backbone oriented in the edge-on manner on the substrate. **PBDTD4T** also showed a weak lamellar diffraction along the q_{xy} axis, indicating the existence of some crystallites with the face-on backbone orientation. The polymer thin films also yielded a strong diffraction along the q_{xy} axes at q_{xy} = 1.76−1.80, which corresponds to the π-stacking structure, (010). The π-stacking distances of the polymers are around 3.5−3.6 Å, which are narrow for π-conjugated polymers. This indicates that these
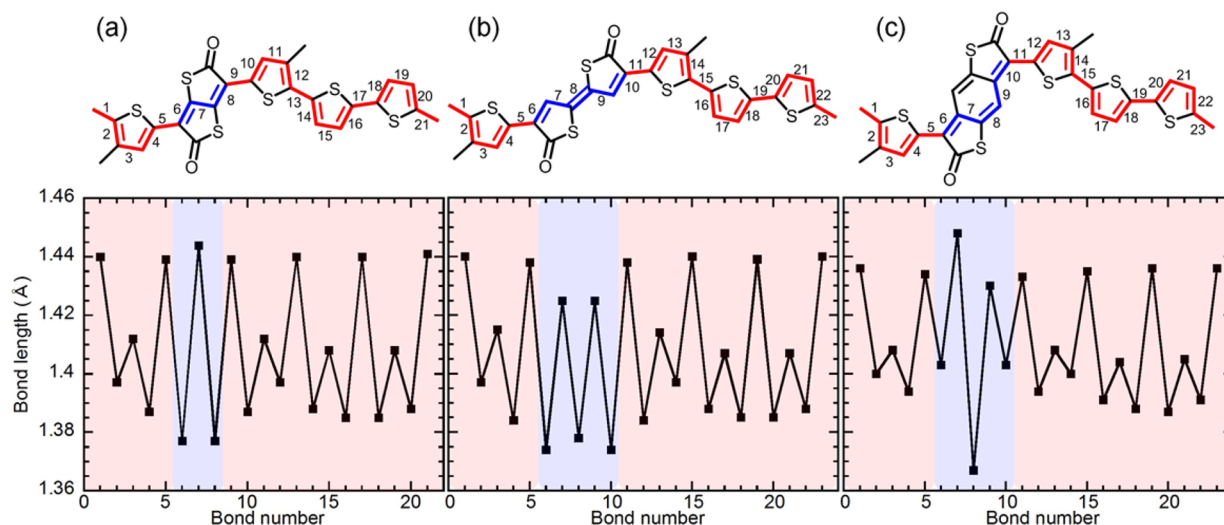
Figure 7. Chemical structures of polymer repeat units with carbon–carbon bond numbers (upper) and plots of carbon–carbon bond length at the respective bond number (lower) for **PTTD4T** (a), **PBTD4T** (b), and **PBDTD4T** (c). The bond lengths were extracted from the central repeat unit of the trimer model optimized by the DFT method at the B3LYP/6-31G(d) level.
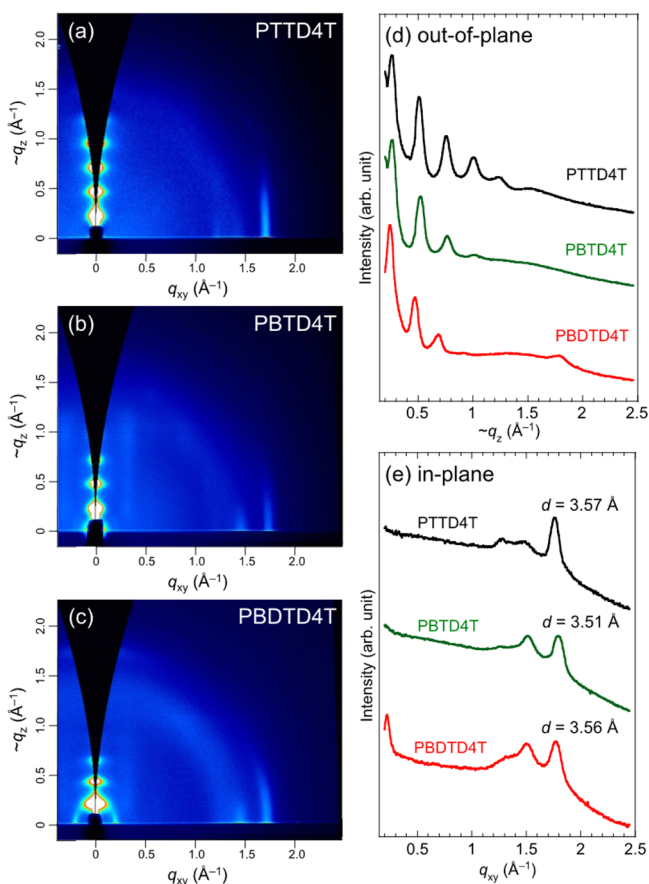
Figure 8. (a–c) 2D-GIXD images of annealed polymer thin films: (a) PTTD4T, (b) PBTD4T, and (c) PBDTD4T. (d–e) Diffraction profiles extracted from the 2D-GIXD images: (d) in-plane (along the q_{xy} axis) and (e) out-of-plane (along the quasi-q_z axis).

thienoquinoidal units lead to strong intermolecular interactions when incorporated in the π-conjugated polymer backbone.

Charge Transport Property. Charge transport property is one of the most important characteristics of π-conjugated polymers for application in organic devices. We here evaluated

the charge transport properties of **PTTD4T**, **PBTD4T**, and **PBDTD4T** by fabricating their OFET devices. Bottom-gate top-contact OFET devices were fabricated by spin-coating the polymer solutions. Figure 9 presents the typical output and transfer curves of the devices. All the devices based on these polymers showed good saturation behavior in the output curves as well as V-shaped transfer curves in the saturation regime under both p- and n-channel operations, which are typical of ambipolar OFETs. The mobilities indicated very small gate-voltage dependence (Figure S17).

All the polymers in this study exhibited relatively high hole and electron mobilities (Table 3). In particular, newly synthesized **PBTD4T** and **PBDTD4T** had more balanced hole and electron mobilities (μ_h and μ_e) than **PTTD4T**. **PBTD4T** showed $\mu_h = 0.16$ cm^2 V^{-1} s^{-1} and $\mu_e = 0.16$ cm^2 V^{-1} s^{-1}, and **PBDTD4T** showed $\mu_h = 0.30$ cm^2 V^{-1} s^{-1} and $\mu_e = 0.35$ cm^2 V^{-1} s^{-1}, whereas **PTTD4T** showed $\mu_h = 0.34$ cm^2 V^{-1} s^{-1} and $\mu_e = 0.16$ cm^2 V^{-1} s^{-1}. Thus, the electron-to-hole mobility ratios (μ_e/μ_h) for **PTTD4T**, **PBTD4T**, and **PBDTD4T** were 0.47, 1.00, and 1.17, respectively. This meant that extending the π-conjugation of the thienoquinoidal unit enhanced the n-channel character. This could be explained by the geometry of the LUMOs that are dominantly located on the thienoquinoidal units in these polymers. The polymers with larger thienoquinoids have denser LUMOs along the backbone (Figures S14 and S15). This would likely result in the more efficient intermolecular LUMO–LUMO interactions, leading to the enhanced n-channel character and balanced hole and electron mobilities.

■ CONCLUSIONS

We have synthesized novel π-conjugated polymers incorporating thienoquinoidal acceptor units BTD and BDTD, namely, **PBTD4T** and **PBDTD4T**. **PBTD4T** yielded a deep LUMO energy level of −3.77 eV and a small bandgap of 1.28 eV, both of which are similar to those of **PTTD4T**. Interestingly, **PBDTD4T** showed a much deeper LUMO energy level of −4.04 eV and a much smaller bandgap of 0.88 eV compared to those of **PTTD4T** and **PBTD4T**. Furthermore, **PBDTD4T** exhibited quite high transparency in the visible region. The
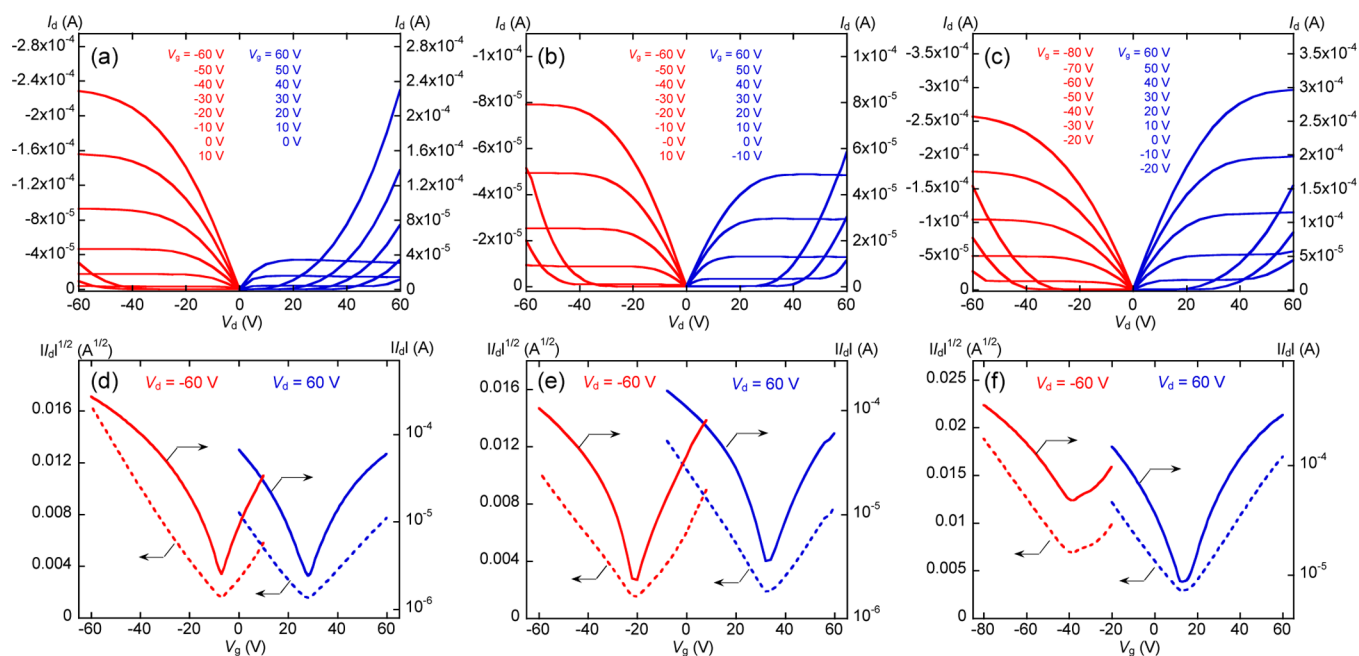
Figure 9. Typical output and transfer curves of the OFET devices based on **PTTD4T** (a and d), **PBTD4T** (b and e), and **PBDTD4T** (c and f), respectively. Red and blue lines correspond to data measured under p- and n-channel operations, respectively.

Table 3. Charge Transport Properties of Polymers Evaluated as OFETs

polymer	μ_h (cm^2 V^{-1} s^{-1})[a]	$V_{th,h}$ (V)[b]	μ_e (cm^2 V^{-1} s^{-1})[c]	$V_{th,e}$ (V)[d]	μ_e/μ_h[e]
PTTD4T	0.34 [±0.08]	−6.3 [±1.6]	0.16 [±0.04]	21.0 [±1.2]	0.47
PBTD4T	0.16 [±0.02]	−16.1 [±2.0]	0.16 [±0.02]	27.5 [±2.5]	1.00
PBDTD4T	0.30 [±0.06]	−18.0 [±1.3]	0.35 [±0.06]	7.0 [±1.0]	1.17

[a]Average hole mobilities. [b]Average threshold voltages for p-type operation. [c]Average electron mobilities. [d]Average threshold voltages for n-type operation. [e]Ratios of electron to hole mobilities. Brackets for all the parameters are standard deviations.

significantly small bandgap of **PBDTD4T** can be rationalized by considering the contribution of the resonance form of the conjugated backbone. In the resonance form with the quaterthiophene moiety in the quinoid structure, the *p*-benzoquinodimethane skeleton in the BDTD unit turns into the aromatic-like structure from the quinoid structure in the primary form. This would stabilize the resonance form in **PBDTD4T** relative to those in **PTTD4T** and **PBTD4T**, which enhances the contribution of the resonance form and thus the overall quinoidal character in **PBDTD4T**. This hypothesis was supported by the difference in bond lengths between **PBDTD4T** and **PTTD4T/PBTD4T** using DFT calculation. In addition, the polymers exhibited air-stable ambipolar charge transport with relatively high mobilities of the order of 10^{-1} cm^2 V^{-1} s^{-1}. Notably, both **PBTD4T** and **PBDTD4T** showed higher electron mobilities and thus more balanced p- and n-channel character than **PTTD4T**.

These results suggest that TTD, BTD, BDTD, and similar thienoquinoidal acceptor units are interesting building units for π-conjugated polymers. Moreover, π-extended quinoids having strong electron-withdrawing groups that include aromatic substructures in the resonance structure can be promising acceptor units for the creation of very small bandgap D−A polymers. We hope that these results will provide new insights into the design of new π-conjugated polymers with high NIR activity and visible transparency as well as high charge carrier mobilities which would be useful for next-generation organic optoelectronic devices.

■ ASSOCIATED CONTENT

ⓢ Supporting Information

The Supporting Information is available free of charge on the ACS Publications website at DOI: 10.1021/jacs.6b03688.

Detailed experimental procedures and characterization of monomers and polymers, as well as additional figures and tables (PDF)

■ AUTHOR INFORMATION

Corresponding Authors

*kohsuke.kawabata@gmail.com
*itaru.osaka@riken.jp

Present Address

K.K.: Department of Chemical and Environmental Engineering, Yale University, New Haven, Connecticut 06511, United States.

Notes

The authors declare no competing financial interest.

■ REFERENCES

(1) Burroughes, J. H.; Bradley, D. D. C.; Brown, A. R.; Marks, R. N.; Mackay, K.; Friend, R. H.; Burns, P. L.; Holmes, A. B. *Nature* **1990**, *347*, 539.

(2) Sirringhaus, H.; Brown, P. J.; Friend, R. H.; Nielsen, M. M.; Bechgaard, K.; Langeveld-Voss, B. M. W.; Spiering, A. J. H.; Janssen, R. A. J.; Meijer, E. W.; Herwig, P.; de Leeuw, D. M. *Nature* **1999**, *401*, 685.

(3) Yu, G.; Gao, J.; Hummelen, J. C.; Wudl, F.; Heeger, A. J. *Science* **1995**, *270*, 1789.

(4) Argun, A. A.; Cirpan, A.; Reynolds, J. R. *Adv. Mater.* **2003**, *15*, 1338.

(5) Jonas, F.; Schrader, L. *Synth. Met.* **1991**, *41*, 831.

(6) Aleshin, A. N.; Williams, S. R.; Heeger, A. J. *Synth. Met.* **1998**, *94*, 173.

(7) Soci, C.; Hwang, I. W.; Moses, D.; Zhu, Z.; Waller, D.; Gaudiana, R.; Brabec, C. J.; Heeger, A. J. *Adv. Funct. Mater.* **2007**, *17*, 632.

(8) Kemp, N. T.; Kaiser, A. B.; Liu, C. J.; Chapman, B.; Mercier, O.; Carr, A. M.; Trodahl, H. J.; Buckley, R. G.; Partridge, A. C.; Lee, J. Y.; Kim, C. Y.; Bartl, A.; Dunsch, L.; Smith, W. T.; Shapiro, J. S. *J. Polym. Sci., Part B: Polym. Phys.* **1999**, *37*, 953.

(9) Dou, L.; Liu, Y.; Hong, Z.; Li, G.; Yang, Y. *Chem. Rev.* **2015**, *115*, 12633.

(10) Bérubé, N.; Gaudreau, J.; Côté, M. *Macromolecules* **2013**, *46*, 6873.

(11) Steckler, T. T.; Henriksson, P.; Mollinger, S.; Lundin, A.; Salleo, A.; Andersson, M. R. *J. Am. Chem. Soc.* **2014**, *136*, 1190.

(12) Gong, X.; Tong, M.; Xia, Y.; Cai, W.; Moon, J. S.; Cao, Y.; Yu, G.; Shieh, C.-L.; Nilsson, B.; Heeger, A. J. *Science* **2009**, *325*, 1665.

(13) Wudl, F.; Kobayashi, M.; Heeger, A. J. *J. Org. Chem.* **1984**, *49*, 3382.

(14) Brédas, J. L.; Heeger, A. J.; Wudl, F. *J. Chem. Phys.* **1986**, *85*, 4673.

(15) Bredas, J. L. *J. Chem. Phys.* **1985**, *82*, 3808.

(16) Kuerti, J.; Surjan, P. R.; Kertesz, M. *J. Am. Chem. Soc.* **1991**, *113*, 9865.

(17) Nayak, K.; Marynick, D. S. *Macromolecules* **1990**, *23*, 2237.

(18) Pomerantz, M.; Chaloner-Gill, B.; Harding, L. O.; Tseng, J. J.; Pomerantz, W. J. *J. Chem. Soc., Chem. Commun.* **1992**, 1672.

(19) Kenning, D. D.; Rasmussen, S. C. *Macromolecules* **2003**, *36*, 6298.

(20) Wen, L.; Duck, B. C.; Dastoor, P. C.; Rasmussen, S. C. *Macromolecules* **2008**, *41*, 4576.

(21) Havinga, E. E.; ten Hoeve, W.; Wynberg, H. *Polym. Bull. (Heidelberg, Ger.)* **1992**, *29*, 119.

(22) Kitamura, C.; Tanaka, S.; Yamashita, Y. *Chem. Mater.* **1996**, *8*, 570.

(23) Beaujuge, P. M.; Amb, C. M.; Reynolds, J. R. *Acc. Chem. Res.* **2010**, *43*, 1396.

(24) Zhou, E.; Hashimoto, K.; Tajima, K. *Polymer* **2013**, *54*, 6501.

(25) Li, M.; An, C.; Marszalek, T.; Guo, X.; Long, Y.-Z.; Yin, H.; Gu, C.; Baumgarten, M.; Pisula, W.; Müllen, K. *Chem. Mater.* **2015**, *27*, 2218.

(26) van Pruissen, G. W. P.; Pidko, E. A.; Wienk, M. M.; Janssen, R. A. J. *J. Mater. Chem. C* **2014**, *2*, 731.

(27) Kang, I.; Yun, H.-J.; Chung, D. S.; Kwon, S.-K.; Kim, Y.-H. *J. Am. Chem. Soc.* **2013**, *135*, 14896.

(28) Zhou, E.; Nakano, M.; Izawa, S.; Cong, J.; Osaka, I.; Takimiya, K.; Tajima, K. *ACS Macro Lett.* **2014**, *3*, 872.

(29) Gao, L.; Zhang, Z.-G.; Xue, L.; Min, J.; Zhang, J.; Wei, Z.; Li, Y. *Adv. Mater.* **2016**, *28*, 1884.

(30) Fabiano, S.; Chen, Z.; Vahedi, S.; Facchetti, A.; Pignataro, B.; Loi, M. A. *J. Mater. Chem.* **2011**, *21*, 5891.

(31) Li, W.; Hendriks, K. H.; Wienk, M. M.; Janssen, R. A. J. *Acc. Chem. Res.* **2016**, *49*, 78.

(32) Yan, H.; Chen, Z.; Zheng, Y.; Newman, C.; Quinn, J. R.; Dotz, F.; Kastler, M.; Facchetti, A. *Nature* **2009**, *457*, 679.

(33) Guo, X.; Facchetti, A.; Marks, T. J. *Chem. Rev.* **2014**, *114*, 8943.

(34) Stalder, R.; Mei, J.; Reynolds, J. R. *Macromolecules* **2010**, *43*, 8348.

(35) Lei, T.; Wang, J.-Y.; Pei, J. *Acc. Chem. Res.* **2014**, *47*, 1117.

(36) Rumer, J. W.; Levick, M.; Dai, S.-Y.; Rossbauer, S.; Huang, Z.; Biniek, L.; Anthopoulos, T. D.; Durrant, J. R.; Procter, D. J.; McCulloch, I. *Chem. Commun.* **2013**, *49*, 4465.

(37) Cui, W.; Wudl, F. *Macromolecules* **2013**, *46*, 7232.

(38) Fan, J.; Yuen, J. D.; Cui, W.; Seifter, J.; Mohebbi, A. R.; Wang, M.; Zhou, H.; Heeger, A.; Wudl, F. *Adv. Mater.* **2012**, *24*, 6164.

(39) An, C.; Li, M.; Marszalek, T.; Li, D.; Berger, R.; Pisula, W.; Baumgarten, M. *Chem. Mater.* **2014**, *26*, 5923.

(40) Chen, S.; Bolag, A.; Nishida, J.-i.; Yamashita, Y. *Chem. Lett.* **2011**, *40*, 998.

(41) Suzuki, Y.; Miyazaki, E.; Takimiya, K. *J. Am. Chem. Soc.* **2010**, *132*, 10453.

(42) Li, J.; Qiao, X.; Xiong, Y.; Li, H.; Zhu, D. *Chem. Mater.* **2014**, *26*, 5782.

(43) Mori, T.; Yanai, N.; Osaka, I.; Takimiya, K. *Org. Lett.* **2014**, *16*, 1334.

(44) Wu, Q.; Ren, S.; Wang, M.; Qiao, X.; Li, H.; Gao, X.; Yang, X.; Zhu, D. *Adv. Funct. Mater.* **2013**, *23*, 2277.

(45) Handa, S.; Miyazaki, E.; Takimiya, K.; Kunugi, Y. *J. Am. Chem. Soc.* **2007**, *129*, 11684.

(46) Chesterfield, R. J.; Newman, C. R.; Pappenfus, T. M.; Ewbank, P. C.; Haukaas, M. H.; Mann, K. R.; Miller, L. L.; Frisbie, C. D. *Adv. Mater.* **2003**, *15*, 1278.

(47) Osaka, I.; Abe, T.; Mori, H.; Saito, M.; Takemura, N.; Koganezawa, T.; Takimiya, K. *J. Mater. Chem. C* **2014**, *2*, 2307.

(48) Kawabata, K.; Osaka, I.; Nakano, M.; Takemura, N.; Koganezawa, T.; Takimiya, K. *Adv. Electron. Mater.* **2015**, *1*, 1500039.

(49) Nakatsuka, M.; Nakasuji, K.; Murata, I.; Watanabe, I.; Saito, G.; Enoki, T.; Inokuchi, H. *Chem. Lett.* **1983**, *12*, 905.

(50) Fukazawa, A.; Adachi, M.; Nakakura, K.; Saito, S.; Yamaguchi, S. *Chem. Commun.* **2013**, *49*, 7117.

(51) Schnurch, M.; Spina, M.; Khan, A. F.; Mihovilovic, M. D.; Stanetty, P. *Chem. Soc. Rev.* **2007**, *36*, 1046.

(52) Bijleveld, J. C.; Gevaerts, V. S.; Di Nuzzo, D.; Turbiez, M.; Mathijssen, S. G. J.; de Leeuw, D. M.; Wienk, M. M.; Janssen, R. A. J. *Adv. Mater.* **2010**, *22*, E242.

(53) Osaka, I.; Abe, T.; Shimawaki, M.; Koganezawa, T.; Takimiya, K. *ACS Macro Lett.* **2012**, *1*, 437.

(54) Zhang, G.; Ye, Z.; Li, P.; Guo, J.; Wang, Q.; Tang, L.; Lu, H.; Qiu, L. *Polym. Chem.* **2015**, *6*, 3970.

(55) Foster, M. E.; Zhang, B. A.; Murtagh, D.; Liu, Y.; Sfeir, M. Y.; Wong, B. M.; Azoulay, J. D. *Macromol. Rapid Commun.* **2014**, *35*, 1516.

(56) Van Pruissen, G. W. P.; Gholamrezaie, F.; Wienk, M. M.; Janssen, R. A. J. *J. Mater. Chem.* **2012**, *22*, 20387.

(57) Tautz, R.; Da Como, E.; Limmer, T.; Feldmann, J.; Egelhaaf, H.-J.; von Hauff, E.; Lemaur, V.; Beljonne, D.; Yilmaz, S.; Dumsch, I.; Allard, S.; Scherf, U. *Nat. Commun.* **2012**, *3*, 970.

(58) Takeda, Y.; Andrew, T. L.; Lobez, J. M.; Mork, A. J.; Swager, T. M. *Angew. Chem., Int. Ed.* **2012**, *51*, 9042.

(59) Zhang, H.; Jenatsch, S.; De Jonghe, J.; Nüesch, F.; Steim, R.; Véron, A. C.; Hany, R. *Sci. Rep.* **2015**, *5*, 9439.

(60) Yao, Y.; Liang, Y.; Shrotriya, V.; Xiao, S.; Yu, L.; Yang, Y. *Adv. Mater.* **2007**, *19*, 3979.

(61) Wang, L.; Yoon, M.-H.; Lu, G.; Yang, Y.; Facchetti, A.; Marks, T. J. *Nat. Mater.* **2006**, *5*, 893.

(62) Yuan, Y.; Giri, G.; Ayzner, A. L.; Zoombelt, A. P.; Mannsfeld, S. C. B.; Chen, J.; Nordlund, D.; Toney, M. F.; Huang, J.; Bao, Z. *Nat. Commun.* **2014**, *5*, 3005.